Removal behaviors and fouling mechanisms of charged antibiotics and nanoparticles with forward osmosis membrane

Sang-Hun Oh[1], Sanghyun Jeong[1], In Soo Kim[2], Ho Kyong Shon[3], Am Jang[1]*

[1]Graduate School of Water Resources, Sungkyunkwan University (SKKU), 2066 Seobu-ro, Jangan-gu, Suwon-si, Gyeonggi-do, 16419, Republic of Korea

[2]Global Desalination Research Center (GDRC), School of Earth Sciences and Environmental Engineering, Gwangju Institute of Science and Technology (GIST), 123 Cheomdangwagi-ro, Buk-gu, Gwangju, 61005, South Korea

[3] School of Civil and Environmental Engineering, University of Technology Sydney (UTS), City Campus, Broadway, NSW 2007, Australia

*Corresponding author: Tel.: +82-31-290-7526, Fax: +82-31-290-7549, E-mail: amjang@skku.edu

Abstract

Forward osmosis (FO) process was operated with a feed solution (FS) containing charged antibiotics (ABs) and nanoparticles (NPs). The fouling and rejection mechanisms of both charged ABs and NPs were determined experimentally using a negatively-charged polyamide thin film composite FO flat sheet membranes. Two types of ABs and NPs were selected as positively and negatively charged foulants at pH 8. The ABs did not cause significant membrane fouling, but the extent of fouling and rejection changed based on the electrostatic attraction or repulsion forces. The occurrence of electrostatic attraction upon addition of oppositely charged ABs and NPs resulted in membrane flux decline and improvement in rejection efficiency of ABs. On the other hand, mixing of like-charged

ABs and NPs generated repulsive forces that improved rejection efficiency but made no changes to the membrane flux. Additionally, NPs and ABs were mixed and tested at various concentrations and pH levels to rectify the behavior of ABs. The aggregate size and removal efficiency was observed to vary with the change in the electron double layer of the mixture. The results obtained from this study can provide useful insights for developing strategies to treat or control ABs or charged foulants in the FO process.

Keywords: Antibiotics; Electron double layer; Forward osmosis; Nanoparticles

1. Introduction

In order to achieve better treatment efficiency and reduce negative environmental impacts, wastewater treatment technologies are being developed continuously. Membrane technologies, such as ultrafiltration (UF), nanofiltration (NF)[1] and reverse osmosis (RO)[2] are being extensively used for controlling wastewater quality [3]. However, these membrane processes require high pressure to operate and suffer from severe membrane fouling [4, 5].

In this regard, forward osmosis (FO) is proposed as an alternative wastewater treatment process that requires little or no pressure compared to other pressurized membrane technologies (i.e., UF, NF, RO)[6]. FO processes use the osmotic pressure gradient as the driving force to separate pure water from the FS (i.e., wastewater). In addition, FO has other advantages, such as less energy-intensive, lower membrane fouling propensity and easier fouling removal compared to other pressure-driven membrane processes [7, 8]. The main issue of the FO process in wastewater treatment is still membrane fouling [9]. Several studies have investigated various measures to eliminate or mitigate membrane fouling in the FO process. Several contaminants like organic, particulate, trace pollutants and nutrients contained in the wastewater still threaten the membrane process [10-13]. As a result, pretreatment of source water and chemical cleaning of membranes are required to reduce membrane fouling, but they incur additional cost and increase energy consumption.

There are various approaches to understand the membrane fouling process, such as pollutant removal mechanisms [11, 14-16], process optimization [17, 18], etc. The charge effect that occurs in all types of membranes is an interesting factor for fouling studies, which also influences the filtration performance. A previous study evaluated the performance of a polyamide-imide (PAI) hollow fiber membrane [19] that demonstrated high water permeability and salt rejection. The charges in the densely active membrane surface were found to impose a repulsive force on salt penetration through the membrane. Another study investigated the FO process with a thin-film composite membrane for

77 separation of tetracycline from aqueous solution, which indicated that the change in pH affected the
78 foulants' polarity. The ion rejection rate was found to increase when the polarity of the membrane and
79 foulants were same due to the repulsive force. Margarida et al. [20] observed that the negative charge
80 of the membrane increased with increasing pH, which caused flux decline but improved ion rejection.
81 The membrane was less negatively charged for divalent hardness ions ($CaCl_2$ and $MgSO_4$) with more
82 severe flux decline. These results indicate that foulants in wastewater respond differently depending
83 on the charge, and this behavior can be utilized to control membrane fouling.

84 Our previous study [15] also investigated the effect of the membrane's surface charge on
85 membrane flux and ion rejection using charged nanoparticles (NPs) in the FS for FO process.
86 Interestingly, the particle-fouling phenomenon and filtration performance differed significantly with
87 the charge of the NPs. Positively charged NPs (PNPs) showed low water flux due to the electrostatic
88 attraction between the membrane and the NPs. Thus, the formation of a dense and thick fouling layer
89 was observed. However, when negatively charged NPs (NNPs) were applied to the same charged
90 membrane surface, electrostatic repulsion between NPs and membrane occurred. As the electrostatic
91 force occurs in the direction opposite to osmotic pressure, the presence of NNPs reduced the formation
92 of the fouling layer [15].

93 Recent studies investigated the treatment of antibiotics (ABs), which are one of the emerging
94 micropollutants. The emergence of ABs in water has drawn a great deal of attention because of the
95 induced AB-resistance genes, which are seriously harmful to human health and ecological security
96 [21-23]. Although some studies proposed strategies to control the ABs by membrane
97 processes(reference?) , there are few studies on the characteristics of ABs in the FO process
98 (reference?). In particular, no mechanism study exists on materials that are difficult to remove by
99 conventional wastewater treatment (i.e., NPs and ABs) when they enter into the FO process.

100 This study aims to evaluate the performance of the FO process when ABs are present in FS by

investigating the characteristics of ABs under different charge conditions. The removal efficiency and water flux were evaluated when ABs with same or different polarities at a given pH were used. In addition, the rejection mechanism was developed by studying the interaction between the ABs and NPs. Fouling behavior on the membrane surface was investigated using a mixture of NPs or/and ABs in the wastewater.

2. Materials and Methods

2.1. Charged NPs, ABs, and FO membrane

Zinc oxide (ZnO) and silicon dioxide (SiO_2) were used as PNPs and NNPs, respectively. The sizes of both NPs ranged between 20–40 nm and their purity was 99.5%. The ABs used in this study were sulfasalazine and amoxicillin trihydrate, which are categorized as a positively charged ABs (PAB) and negatively charged ABs (NAB), respectively. The zeta potentials of the NPs and ABs as a function of pH are shown in **Fig. S1** (Supplementary Information). At pH 8.0 (which is the operating condition), the zeta potentials of the NPs and ABs are as follows: SiO_2 = -48.17 mV, ZnO = 38.06 mV, amoxicillin trihydrate = -37.23 mV, and sulfasalazine = 35.16 mV. The NPs and ABs used in this study were selected as materials whose charges are opposite to each other and whose absolute values of the zeta potential are similar. All the NPs and ABs were purchased from Sigma-Aldrich. The ABs were in powder form and their solubility was 1 mg/mL (PAB) and 3.4 mg/mL (NAB). The FO membrane (Porifera, CA, USA) was a polyamide (PA)-based thin-film composite (TFC) membrane, and the effective membrane area used in the experiment was 20.02 cm^2. More detailed characteristics of the FO membrane can be found elsewhere [13].

2.2 FO performance with charged NPs and AB

FS was prepared by mixing 2.5 mg of NPs and 2.5 mg of ABs in deionized (DI) water using eight different combinations: 1) NNPs, 2) PNPs, 3) NAB, 4) PAB, 5) NNPs + NAB, 6) NNPs + PAB, 7) PNPs + NAB, and 8) PNPs + PAB), and its pH was kept around 8.0. The draw solution (DS) was

prepared as 0.5 M NaCl. The initial volume of both FS and DS was maintained at 1 L. Both FS and DS were circulated at a cross-flow velocity of 8.55 cm/s inside the FO membrane module using a gear pump (Longer Pump WT3000-1FA, China). A chiller was used to (CPT Inc., Republic of Korea) regulate the temperature of FS and DS at 25±0.5°C. The weight of DS was measured using a digital balance (AND GF-6000, NY, USA) at recorded at a one-minute interval.

A UV spectrophotometer (DR-6000, CO, USA) was used to analyze the rejection rate of the ABs. The spectra were measured at wavelengths between 0 and 500 to calculate the concentration of AB. A straight-sided cuvette with a lid of 12.5 mm × 12.5 mm × 4.5 mm was used. The control sample was used as 5 mg/L of AB solution (100 mL). The samples that were tested included: initial FS, FS and DS collected immediately after the experiment and extracted solution from the used membrane. At the end of the experiment, ABs attached to the membrane were extracted using the following steps: membrane samples were loaded into a beaker containing 1 L of DI water and shaken for 24 h at 150 rpm. Then 1 mL of the sample was placed in a disposable cuvette for UV analysis. The spectrum of the sample was measured at the spectral ranges provided by the manufacturer.

2.3. Interaction between ABs and NPs

2.3.1 ABs to NPs

In order to determine the interaction between ABs and NPs, which is essential to understand the behaviors of charged ABs and NPs in the FO process, the change in the concentration of the ABs with NPs was measured over time. The interaction between ABs and NPs is usually due to their electron double layers. In the water, both ABs and NPs have an electron layer, and the interaction between their electron layers can be changed with particle aggregation [24-26] and zeta potential change [25]. In addition, ABs and NPs exist in different states when in water (AB: ionized, NP: solid). Experiments were conducted to investigate whether they cause the same effect in other conditions. The effects of pH and external ion concentration on the agglomeration size and zeta potential of the mixture

were investigated.

A 2 mg/L NP solution was prepared and sonicated for 30 min to disperse the NPs with an ultrasonic bath (HWASHIN Inc., POWERSONIC410, Republic of Korea) prior to use. Then the ABs were mixed into deionized (DI) water (100 mL) at concentrations of 0, 5, 15, and 30 mg/L. A 50 mL sample of each of the prepared NPs and ABs were mixed and agitated thoroughly for 30 min using a magnetic stirrer. A 1-mL sample was extracted from the mixed solution at every 5 min interval with a disposable syringe. The zeta potential and particle size of the samples were measured by using size and zeta potential analyzer (Microtrac Inc., Nanotrac3, CA, USA). These measurements were automatically stored and 10 measurements were taken for each sample in particle-size and zeta-potential mode.

2.3.2 Aggregation of NPs influenced by ABs at different pH

At different pH values, the aggregation of NPs with time was analyzed by measuring the particle size distribution. A 20-mg/L NP solution was titrated from pH 3 to pH 9 using 0.1 N-NaOH and 0.1 N-HCl solutions. For the analysis, 0.98 mL of the titrated NP solution and 0.02 mL of the AB solution were mixed.

2.4 Membrane surface morphology

After the end of the operation, the membrane surface morphology was observed using scanning electron microscopy (SEM, SEC, Republic of Korea) for analyzing the foulants on the membrane surface. The membrane sample was washed with DI water to remove the residual FS from the membrane. Then it was dried in an oven at 50°C for 5 h and stored in a desiccator at room temperature for further analysis.

3. Results and discussion

3.1 Flux variation with charged ABs and NPs in the FO process

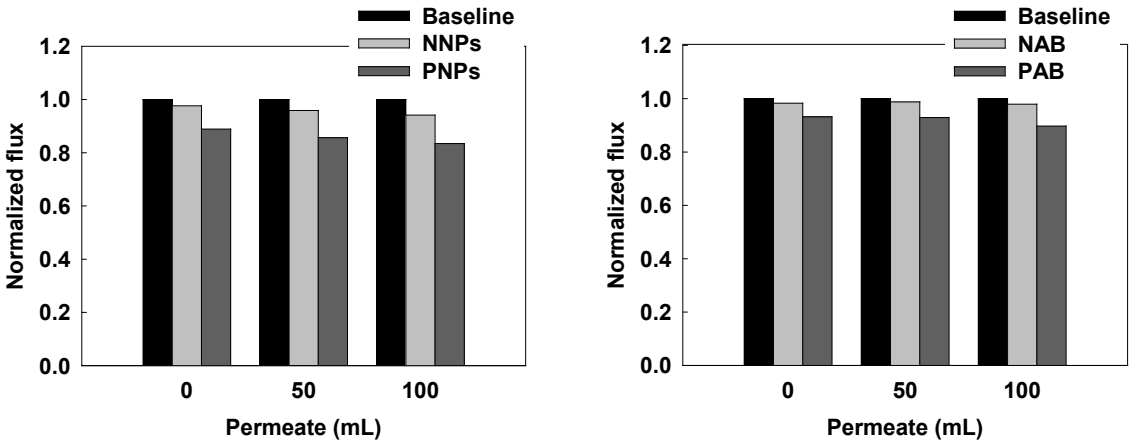

(a) (b)

172 **Fig. 1.** Normalized water flux in the FO process with charged (a) NPs and (b) ABs. (Baseline test was

173 performed with DI water; ~~concentration of NPs; and concentration of ABs~~)

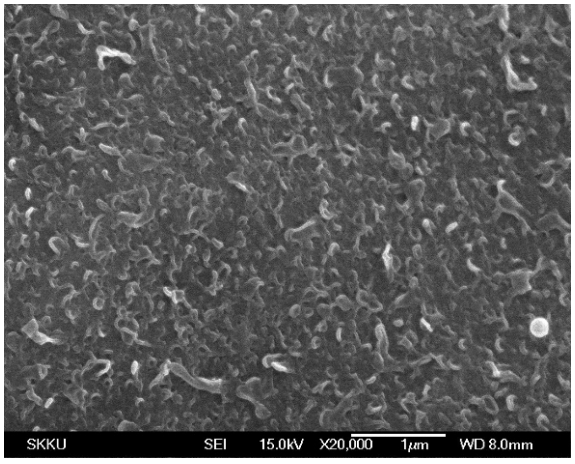

(a) Virgin

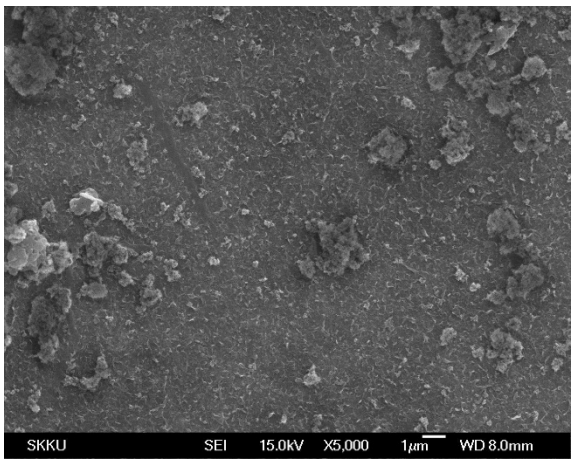

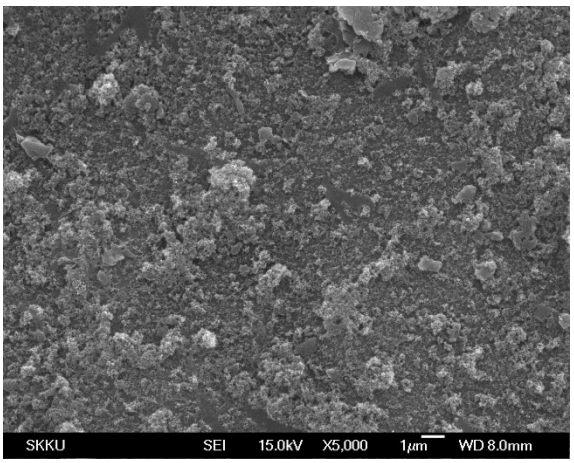

(b) NNPs (c) PNPs

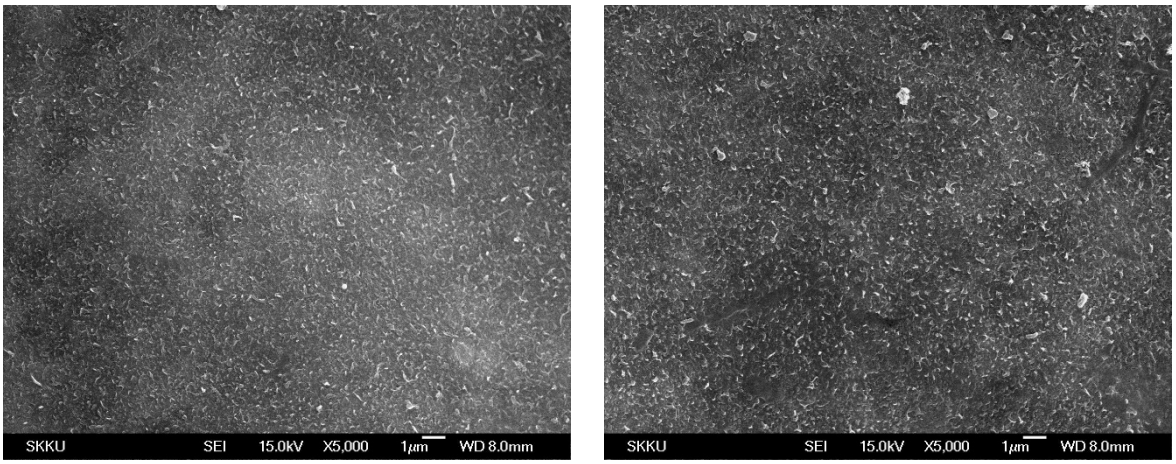

(d) NABs (e) PABs

Fig. 2. SEM images (top surface) of fouled FO membranes with charged NPs and ABs: (a) Virgin, (b) NNPs, (c) PNPs, (d) NABs, and (e) PABs.

As can be seen from **Fig. 1**, the FO flux decreased when charged NPs and ABs were used in FS compared to the baseline study. This is due to the pore-blocking and dilution effect of DS with time. When FO was operated with NPs, the decrease in water flux was higher with PNPs than with NNPs (**Fig. 1a**). The FO flux decreased to less than 5% with NNPs when compared to that of the baseline test. However, PNPs reduced the water flux by more than 12% than that of the baseline test. This can be explained with the effect of the electrostatic force between differently charged NPs and the membrane. In the case of NNPs, there will be electrostatic repulsion between the NNPs and negatively charged membrane surfaces; whereas, the electrostatic attraction may occur between the PNPs and the negatively-charged membrane surface.

The charged ABs also resulted in a decline in FO flux like the NPs (**Fig. 1b**). However, the effect of ABs on flux decline was lesser compared to the NPs. When the NAB is contained in the FS, the flux decline was about 3% compared to baseline flux. PAB caused more flux reduction than NAB due to the electrostatic attraction with the membrane. Because ABs are ionic substances, it is difficult to consider that the flux reduction was not due to aggregation, unlike NPs. PABs may accumulate on

190 the membrane surface due to electrostatic attraction and osmotic pressure on the active layer of the
191 membrane, which may cause further water flux decline by concentration polarization on the membrane
192 surface [27].

193 The PA-based FO membrane used in the experiment shows a ridge-and-valley structure (**Fig.**
194 **2a**). This membrane has a high surface roughness, similar to other pressurized RO and NF membranes,
195 but shows higher chemical resistance, membrane flux and salt rejection [28]. When NPs were used in
196 the FS of the FO process, the ridge-and-valley structures of the membranes disappeared in some or
197 most of the membrane areas confirming that fouling by NPs occurred during the FO process. The
198 membrane operated with NNPs (**Fig. 2b**) showed lower fouling compared to the one operated with
199 PNPs. It is considered that NNPs could not approach the membrane surface as easily as the PNPs
200 because of the electrostatic repulsion of NNPs to the membrane surface; consequently, a loosely bound
201 fouling layer was formed on the membrane surface. On the other hand, PNPs completely covered the
202 membrane surface due to electrostatic attraction, resulting in the loss of the ridge-and-valley structure
203 of the virgin membrane. It is considered that the electron double layer formed by the polymeric
204 membrane affected the aggregation or dispersion of charged NPs on its surface.

205 **Figs. 2d** and **2e** show SEM images of the membranes after the end of FO operation with NAB
206 and PAB, respectively. Unlike NPs, at the end of the process, the membrane was not significantly
207 contaminated with ABs, and the structure of the PA membrane seemed to be the same as that of the
208 virgin membrane. The ABs did not create an invisible fouling layer because they are present in the
209 ionic state in the FS. However, as can be seen from the flux decline pattern in **Fig. 1b,** their effects
210 should be investigated in the FO process.

211 **3.2 FO flux with a mixture of ABs and NPs**

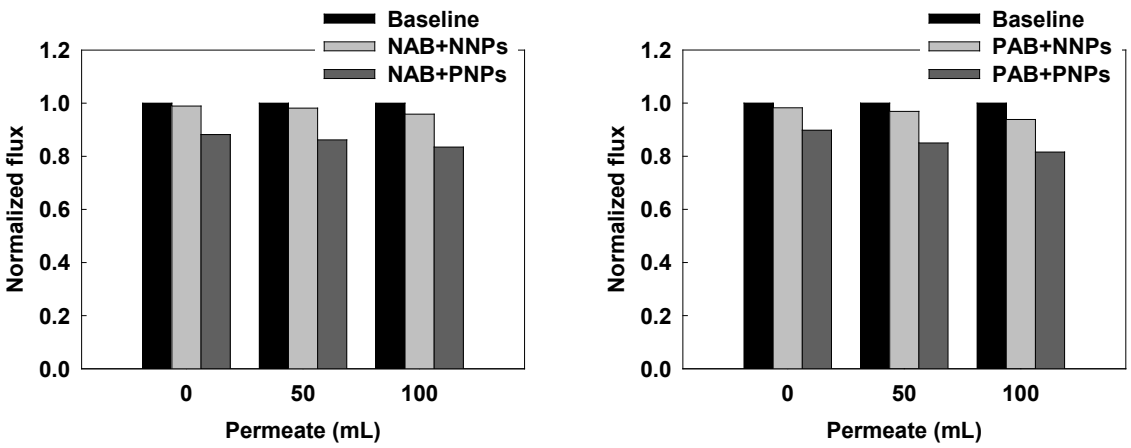

212 **Fig. 3.** Flux variation with a mixture of (a) NAB and NPs and (b) PAB and NPs in the FS.

213 The FO flux decline behavior observed with ABs/NPs mixtures in FS was slightly different
214 from that observed with individual ABs and NPs. When both negatively charged ABs and NPs are used
215 (NAB + NNPs), about 3% of reduction was observed compared to the baseline test (**Fig. 3a**). NAB +
216 NNPs may cause electrostatic repulsion within the FS, and with the negatively-charged membrane
217 surface. This phenomenon can prevent fouling of the membrane surface and minimize flux reduction
218 [23]. However, the flux decreased by approximately 12% with NAB + PNPs (**Fig. 3a**) due to the
219 occurrence of electrostatic attraction between the NAB and PNPs in the FS. The electron double layer
220 of the PNPs reduce and approaches neutrality when NABs attach to them. The PNPs that are charge-
221 neutralized by NABs cause membrane fouling by osmotic pressure, while the remaining PNPs decline
222 flux by attaching to the negatively-charged membrane by electrostatic force.

223 As shown in **Fig. 3b**, FS with PAB + NNPs and PAB + PNPs decreased the flux by 7% and
224 14%, respectively. As observed in Section 3.1, NNPs generate electrostatic repulsion on the membrane
225 surface and PABs generate electrostatic attraction. Although it is difficult to attach to the membrane
226 due to the electrostatic repulsion of the NNPs, the PAB is adsorbed to the NNPs due to electrostatic
227 attraction. This results in a reduction of the NPs' electron double layer, which can be close to neutral
228 and easily attaches to the membrane surface. The reason of flux differences between NAB + PNPs and
229 PAB + NNPs is supported by the reduced absolute zeta potential. PAB+PNPs can be close to the

membrane surface with the electrostatic attraction reducing flux but generating electrostatic repulsion between the PAB and PNPs.

When charged ABs and NPs are used in the FS, their behaviors on the membrane surface are different based on the charge change between the dissolved NPs and ABs. In particular, when the charge between the ABs and NPs is different, the NPs became close to neutrality causing flux decline due to fouling. The removal efficiency in the FO process was measured to observe the changes caused by the ABs attachment during the neutralization of NPs.

3.3 AB rejection efficiency

Table 1 presents the mass of initial FS and final DS to calculate the AB rejection efficiency with single AB and mixture of ABs and NPs. **Fig. 4a** and **4b** show the results of a single AB and **Fig. 5a** and **5b** represent the change in AB rejection and attachment to the membrane surface in the presence of NPs.

Table 1. Mass of initial FS and final DS, and rejection efficiency with AB and mixture of ABs/NPs

AB	NPs	Initial FS mass (mg)	Final DS mass (mg)	Rejection efficiency (%)
NAB	**w/o any NPs**	2.50	0.19	92
	w/ NNPs	2.46	0.14	94
	w/ PNPs	2.51	0.11	96
PAB	**w/o any NPs**	2.49	0.31	85
	w/ NNPs	2.49	0.12	95
	w/ PNPs	2.51	0.18	94

* w/ and w/o stand for with and without, respectively.

3.3.1 Effect of AB charge

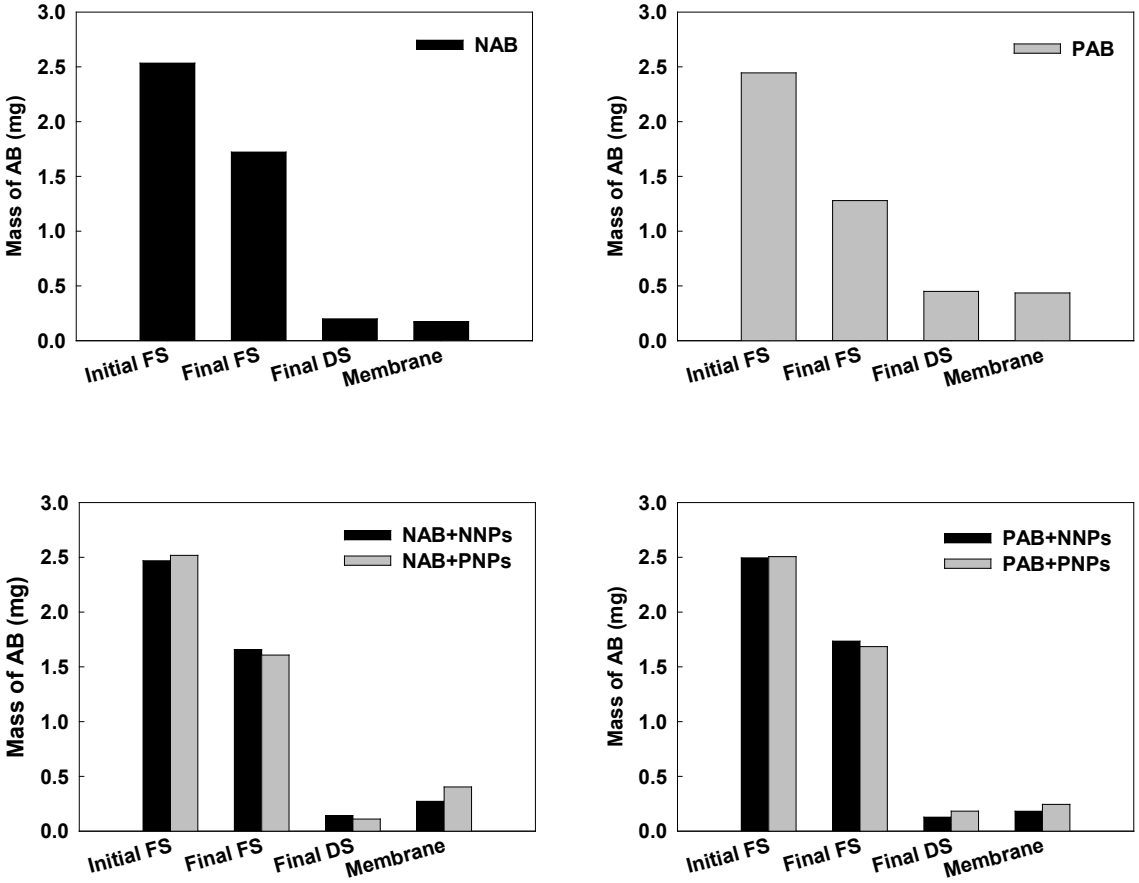

Fig. 4. Mass of individual AB: (a) NAB and (b) PAB. Mass of ABs/NPs mixture: (c) NAB + NPs and (d) PAB + NPs.

In order to compare the removal efficiencies of two differently charged ABs in the FO process, the mass of the ABs in the initial FS, in the final FS and DS, and on the membrane was measured (**Fig. 4**). Based on the AB mass in the initial FS and final DS, the rejection efficiencies of NAB and PAB were 92% and 85%, respectively. In addition, the mass of ABs attached to the membrane could be measured by using UV spectrometer. More PABs (**Fig. 4b**) were present on the membrane than NABs (**Fig. 4a**) because NABs were repelled by the negatively-charged membrane surface, which were partially transmitted at the beginning of the process because of the high osmotic pressure. On the other hand, the PABs attached easily on the membrane surface owing to the existence of electrostatic

attraction between them. In our previous experiment, PNPs formed a fouling layer on the surface of the membrane and created an environment that facilitated easy permeation of DS ions [15]. However, unlike NPs, dissolved ABs appear to permeate easily across the membrane surface without forming a fouling layer. The fouling layer formed by the PABs led to higher transport of PABs from FS to DS by diffusion as a result of higher concentrations of PABs close to the membrane surface (**Fig. 4b**).

3.3.2 Change in AB rejection efficiency with charged NPs

The AB rejection efficiencies and adsorption amounts on the membrane with charged NPs were different from those without NPs. The rejection of NAB + NNPs was similar to that of single NAB due to the existence of electrostatic repulsion between the charged NNPs, NAB and membrane surface. Hence, they had low opportunity to diffuse to DS from FS through the FO membrane. NAB mixed with PNPs showed higher removal efficiency than NAB alone, which is not only due to the repulsive force with the membrane in the presence of NNPs, but also the electrostatic repulsion between the surrounding NNPs and the membrane (**Fig. 4c**). In addition, NAB and PNPs have opposite charges, which causes electrostatic attraction between two. As a result, NAB attached on the PNPs and the thickness of the electronic double layer of the PNPs reduced and became close to neutral. Due to the neutralization of the charges, the mixture (NAB + PNPs) formed a fouling layer on the membrane surface regardless of the electrostatic force of the membrane surface; thereby, reducing the flux. However, the addition of PNPs reduced the concentration of NABs in the FS, and the antifouling layer formed on the membrane surface made it difficult for the ABs to diffuse to the DS, which increased the rejection efficiency.

The results for PAB + NNPs were like those of NAB + PNPs (**Fig. 4d**). As a result of the electrostatic attraction between the two materials, the PAB adsorbed on the NNPs and neutralized their charges. In the presence of PABs, the removal efficiency was low (85%) but the NNPs reduced the fouling layer; consequently, increasing the removal efficiency and decreasing the flux.

In the case of PAB + PNPs, PNPs preferentially accumulated on the membrane surface due to its relatively large physical size and formed an anode layer. The formed anode layer repelled the PABs in the FS when they approached the membrane surface and prevented them from adhering to the PNPs layer. Hence, the flux with PNPs decreased but the removal efficiency increased (**Fig. 4d**).

3.4 Aggregation tendency of ABs with NPs

In order to verify the AB aggregation with NPs, the aggregate size was measured after different concentrations of ABs (0–30 mg/L) were mixed with NPs (20 mg/L, constant) over time (**Fig. 5**). As shown in **Fig. 5a**, PAB concentration increased from 0 to 5 mg/L in the presence of NNPs, and there was little change in the size of the NNPs. Whereas, at 15 and 30 mg/L, the average size gap in the NNPs without PAB increased by about 60 nm. Regardless of PAB concentration, the PNP aggregate size pattern over time was found to be similar (**Fig. 5b**) the charge of NNPs changed at certain concentrations of the PAB (>15 mg/L). In general, it is known that the NPs become neutral when they reach the point zero charge depending on their concentration or when the external state is opposite to the charged state [25]. If the concentration of PAB is much lower than that of the NPs, the size of the electron double layer of the NNPs can be small because the NPs do not reach the neutral state that causes aggregation. Since the PNPs were of the same charge as the injected ABs (**Fig. 5b**), there was no reduction of the electron double layer and the aggregate size constantly increased at all PAB concentrations.

(a) (b)

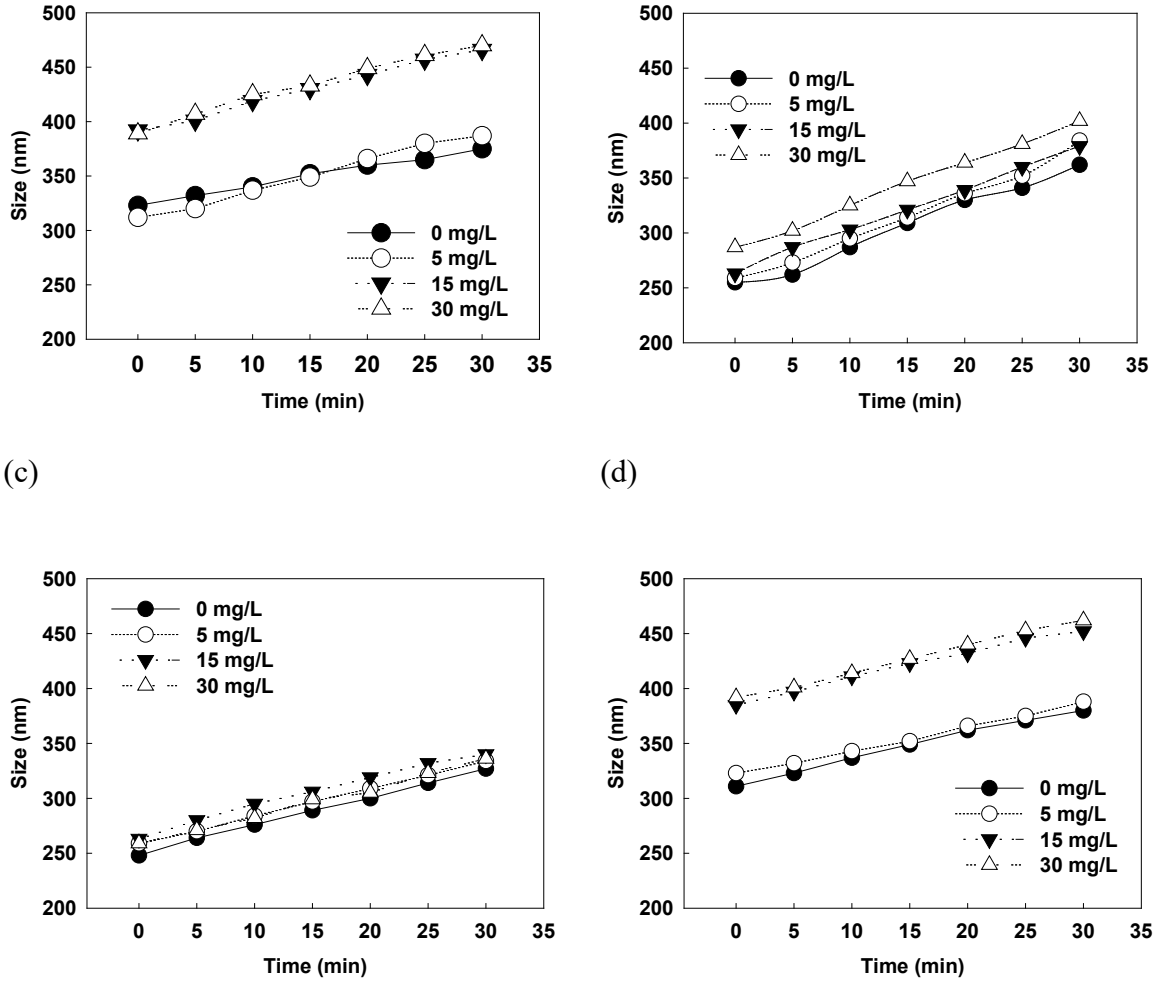

298 **Fig. 5.** Aggregate sizes over time with (a) PAB + NNPs, (b) PAB + PNPs, (c) NAB + NNPs, and (d)
299 NAB + PNPs at pH = 8.

300 **Figs. 5c** and **5d** show the increasing trends in the aggregate size of PAB with NNPs and PNPs,
301 respectively. NAB + NNPs are shown to have a small increase in particle size, similar to that of PAB
302 + PNPs. However, NAB + PNPs had a dramatic increase in aggregate size at a given concentration.
303 As a result, differently charged ABs and NPs increased the aggregate size due to the reduction in the
304 electron double layer.

305 **3.5 Changes in aggregate size at different pH levels**

306 To verify the tendency of aggregation by the change in pH, aggregate sizes were measured in
307 the range of 3.0 to 9.7. As shown in **Fig. 6a**, the aggregate size of NNPs increased by about 65 nm at

pH 3 (the size was maximum at pH 3.0). However, the aggregate size of PNPs increased at pH 9.7 (**Fig. 6b**). The aggregate size of the mixture of NPs and ABs (**Figs. 6c–6f**) was different from that of single NPs. When the charges of both NPs and ABs were the same (**Figs. 6d** and **6e**), changes in the aggregate size were marginal. When the charge between the NPs and ABs was different (**Figs. 6c** and **6f**), the aggregate size increased significantly at pH 8.1 and 9.7 (in alkali condition). This indicates that the aggregation of NPs and ABs depends on pH condition of the FS. To find the relationship between aggregate size and pH, the NPs and the NPs/ABs mixtures were analyzed by changing the pH.

Fig. 7 shows the change in zeta potential of NPs and NPs/ABs mixtures as a function of pH. As shown in **Fig. 7a**, the zeta potential at pH 3, which is the largest pH condition of NNPs aggregate size, was the lowest absolute value of zeta potential among other pH ranges. The PNPs (**Fig. 7b**) also had the lowest absolute value of zeta potential at the maximum aggregate size point (pH 9). In fact, the aggregation and dispersion of the particles are determined by the electrostatic forces (repulsion or attraction) of each other. The particles become stable and aggregation easily occurs at the point in which the zeta potential becomes zero, [29, 30].

The absolute values of the zeta potentials varied for NPs/ABs mixtures with the same charge (NNPs + NAB = 4 mV, and PNPs + PAB = 11 mV). This means that the zeta potentials influenced by the ABs were unstable and could stabilize the NPs [21]. On the other hand, there was certain pH level difference in the zeta potential value where its absolute value is close to zero (NNPs + PAB = pH 9.1, and PNPs + NAB = pH 8.1) in the mixture of oppositely charged materials. It is known that the point of zero charge (PZC), which is the point where the electron double layer of the particle becomes zero, is in a stable state where aggregation can occur easily [25]. This result implies that NPs mixed with ABs of opposite polarity changed the aggregation point due to the change in the PZC of the materials.

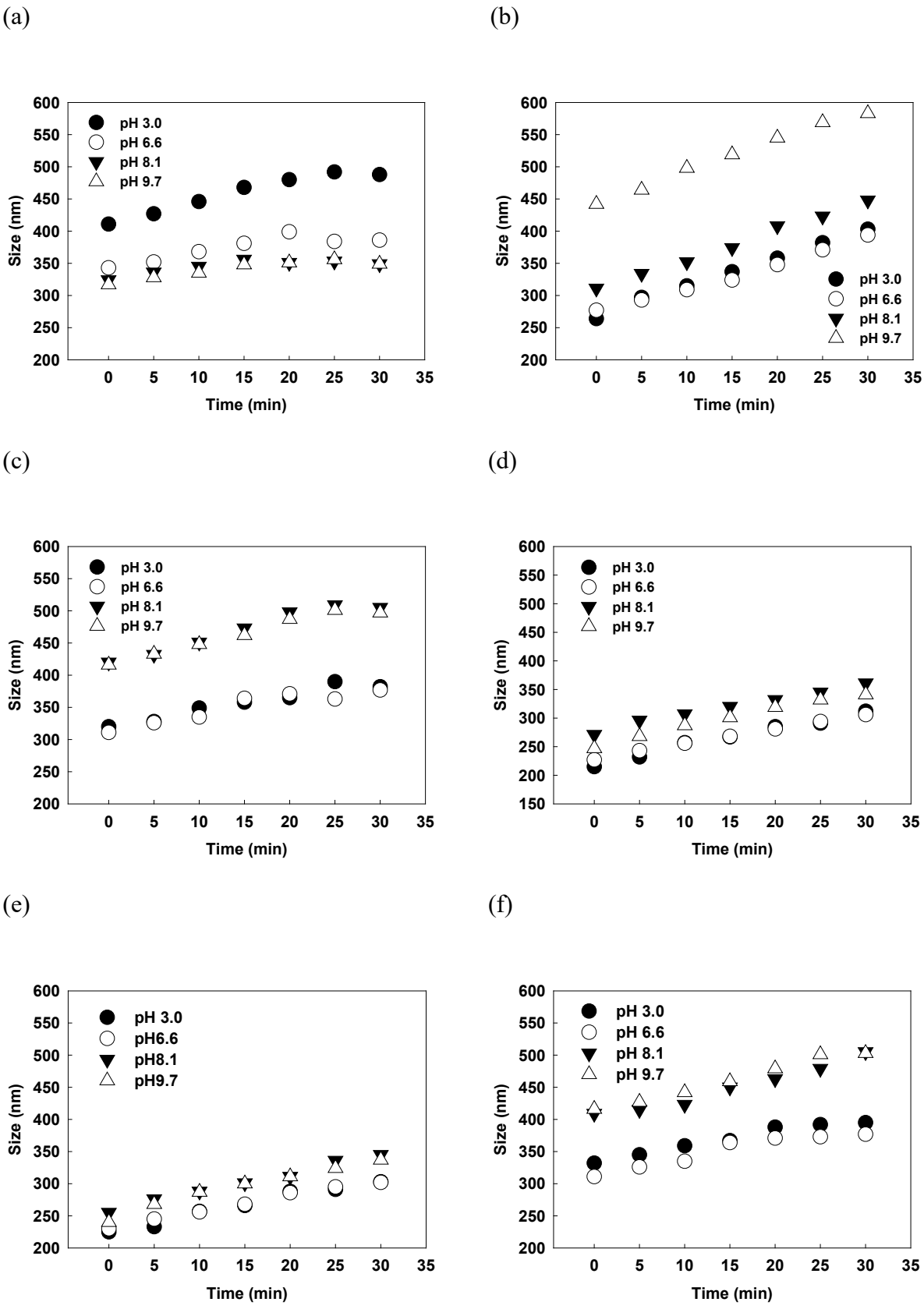

331 **Fig. 6.** Aggregate sizes with time of mixture at various pH conditions: (a) NNPs, (b) PNPs, (c) PAB

332 + NNPs, (d) PAB + PNPs, (e) NAB + NNPs, and (f) NAB + PNPs.

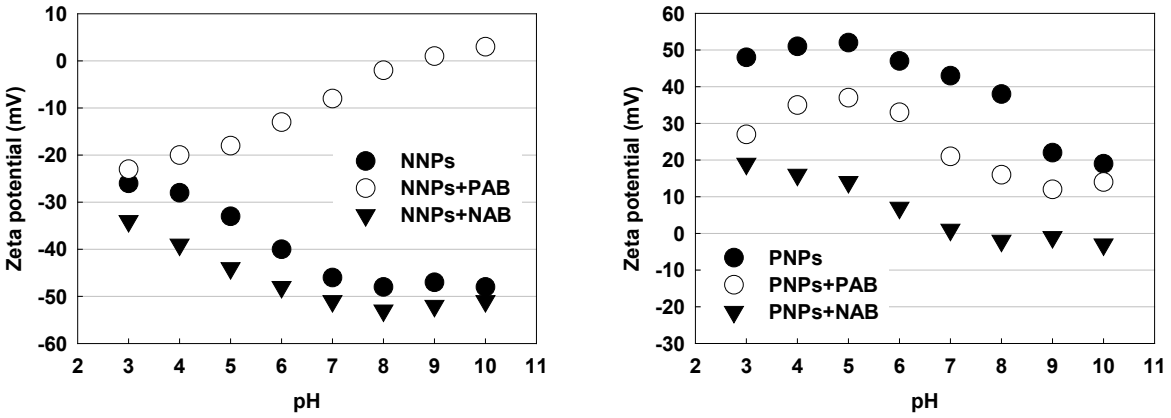

(a) (b)

333 **Fig. 7.** Zeta potentials of (a) NNPs and (b) PNPs without and with ABs as a function of pH.

334 ### 3.6 Rejection mechanism of charged ABs in FO process

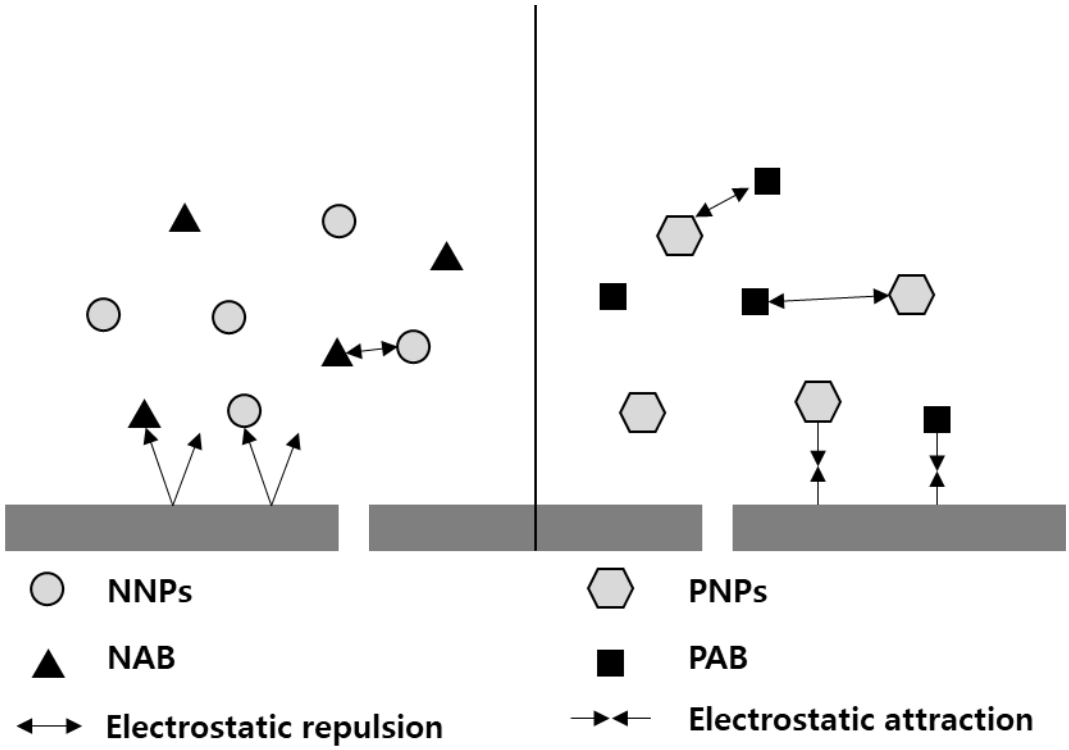

335

336 (a) Electrostatic repulsion of NAB + NNPs

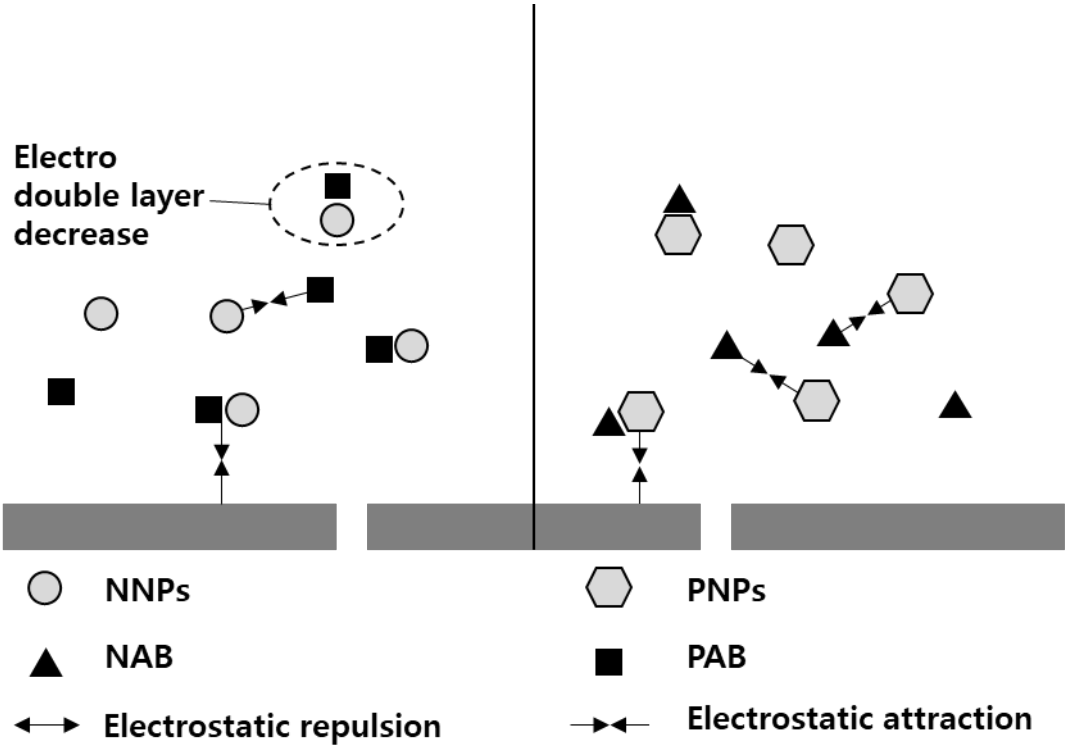

(b) Electrostatic attraction of oppositely charged mixture

Fig. 8. Filtration and fouling mechanisms of charged ABs and NPs in the FO membrane.

The interaction between NPs and ABs can be explained by DVLO theory, which describes the balance between two forces, electrostatic repulsion and Van der Waals attraction. As shown in **Fig. S2** (Supporting Information), the portion of the difference between surface potential and the stern layer is the zeta potential. The change in the zeta potential was altered by decreasing or increasing the thickness of the electron double layer of the material. The electron double layer is changed by the external ion concentration and pH [20, 25, 31]. In the mixed state of NPs and ABs, the ABs exist in an ionic state, and the dissolved ABs act as one of the factors that change the thickness of the electron double layer of the NPs. As the membrane surface remained negatively charged, the membrane performance with NPs/ABs mixture can be determined by the charges of NPs and AB.

Fig. 8 shows the proposed mechanisms of charged ABs and NPs in the FO membrane. First, when the mixed NPs and ABs have the same charge (**Fig. 8a**), an electrostatic repulsive force is

generated between them. The electron double layer of the NPs did not decrease because the same charge existed in the solution. The osmotic pressure in the FO process resulted in the mixture being close to the membrane surface. The mixture adjacent to the membrane experienced a secondary change due to the difference in charge between the ABs/NPs mixture and the membrane. In the case of the same charge, the mixture also experiences a repulsive force with the membrane surface, which makes their adhesion to the membrane surface difficult. However, the membrane and differently charged mixture are easily attached to the membrane due to electrostatic attraction. In this study, PNPs preferentially attached to the membrane due to the charge difference of the material. Attached PNPs formed a fouling layer. The ABs then approached the fouling layer on the membrane surface. However, the fouling layer formed on the membrane surface did not lose its charge resulting it repulsion between ABs and the fouling layer.

Second, if the charge of the mixture is different (**Fig. 8b**), ABs attach to the NPs. The charges of ABs and NPs weaken the charge of the electron double layer of the particles. Due to the decrease in charge, the electron double layer also decreases and the particles approach charge neutrality. NPs that lose their polarity due to the adsorption of ABs become stabilized and aggregate with surrounding NPs; thus, increasing in size. They also attach to the membrane surface by osmotic pressure because the electrostatic force that reacts with the electron double layer of the membrane disappears. ABs were attached to NPs, resulting in a decrease in the total concentration. Moreover, ABs are difficult to transport from FS to DS due to the formation of NPs layer on the membrane surface.

4. Conclusions

This study investigated the effect of charged ABs on the FO performance, the rejection mechanism and the fouling behavior with NPs. The followings results were obtained from this study.

- The formation of the NPs' fouling layer on the membrane changed according to their

electrostatic force. ABs, unlike NPs, did not cause significant membrane contamination but resulted in performance deterioration; low rejection efficiency and concentration polarization near the membrane.

- When ABs were mixed with NPs of opposite charge, the FO flux decreased but the AB rejection efficiency increased. The NPs/ABs mixture with the same charge maintained the flux due to the existence of electrostatic repulsion with the membrane, and the rejection efficiency increased. In the case of electrostatic attraction, the flux decreased, but the rejection efficiency increased.

- To investigate the behavior of ABs, the aggregations of the mixture with NPs were analyzed at various pH levels and concentration conditions. As the electron double layer of the material increased or decreased, the aggregate size of the mixture changed. The rejection efficiency increased under the condition that the charge is the same as that of the membrane, and the aggregate size increased.

- The results imply that when charged materials become neutrally charged, they are easy to clean from the membrane surface. Similarly, ABs can be removed by neutralization. With respect to the surface modification of the membrane, charged NPs could be a useful option to treat the wastewater containing a large amount of charged materials. Removal of ABs and cleaning reversibility should be further investigated.

Acknowledgments

This research was supported by the Basic Science Research Program through the National Research Foundation of Korea (NRF) funded by the Ministry of Science, ICT, & Future Planning (2017R1A2B3009675).

References

[1] L.D. Nghiem, A.I. Schäfer, M. Elimelech, Removal of Natural Hormones by Nanofiltration Membranes: Measurement, Modeling, and Mechanisms, Environmental science & technology, 38 (2004) 1888-1896.

[2] K. Kimura, G. Amy, J. Drewes, Y. Watanabe, Adsorption of hydrophobic compounds onto NF/RO membranes: an artifact leading to overestimation of rejection, Journal of Membrane Science, 221 (2003) 89-101.

[3] E.M.V. Hoek, M. Elimelech, Cake-Enhanced Concentration Polarization: A New Fouling Mechanism for Salt-Rejecting Membranes, Environmental science & technology, 37 (2003) 5581-5588.

[4] Y.C. Kim, S.J. Park, Experimental study of a 4040 spiral-wound forward-osmosis membrane module, Environmental science & technology, 45 (2011) 7737-7745.

[5] R.W. Holloway, L. Miller-Robbie, M. Patel, J.R. Stokes, J. Munakata-Marr, J. Dadakis, T.Y. Cath, Life-cycle assessment of two potable water reuse technologies: MF/RO/UV–AOP treatment and hybrid osmotic membrane bioreactors, Journal of Membrane Science, 507 (2016) 165-178.

[6] T. Xiao, L.D. Nghiem, J. Song, R. Bao, X. Li, T. He, Phenol rejection by cellulose triacetate and thin film composite forward osmosis membranes, Separation and Purification Technology, 186 (2017) 45-54.

[7] C. Boo, M. Elimelech, S. Hong, Fouling control in a forward osmosis process integrating seawater desalination and wastewater reclamation, Journal of Membrane Science, 444 (2013) 148-156.

[8] T. Xiao, P. Dou, J. Wang, J. Song, Y. Wang, X.-M. Li, T. He, Concentrating greywater using hollow fiber thin film composite forward osmosis membranes: Fouling and process optimization, Chemical Engineering Science, 190 (2018) 140-148.

[9] W. Xu, Q. Chen, Q. Ge, Recent advances in forward osmosis (FO) membrane: Chemical modifications on membranes for FO processes, Desalination, 419 (2017) 101-116.

[10] S.-J. Im, H. Rho, S. Jeong, A. Jang, Organic fouling characterization of a CTA-based spiral-wound forward osmosis (SWFO) membrane used in wastewater reuse and seawater desalination, Chemical Engineering Journal, 336 (2018) 141-151.

[11] B. Mi, M. Elimelech, Organic fouling of forward osmosis membranes: Fouling reversibility and cleaning without chemical reagents, Journal of Membrane Science, 348 (2010) 337-345.

[12] S. Lee, C. Boo, M. Elimelech, S. Hong, Comparison of fouling behavior in forward osmosis (FO) and reverse osmosis (RO), Journal of Membrane Science, 365 (2010) 34-39.

[13] Y.-E. Lee, A. Jang, Effect of forward osmosis (membrane) support layer fouling by organic matter in synthetic seawater solution, Desalination and Water Treatment, 57 (2016) 24595-24605.

[14] X. Zhang, J. Tian, S. Gao, W. Shi, Z. Zhang, F. Cui, S. Zhang, S. Guo, X. Yang, H. Xie, D. Liu, Surface functionalization of TFC FO membranes with zwitterionic polymers: Improvement of antifouling and salt-responsive cleaning properties, Journal of Membrane Science, 544 (2017) 368-377.

[15] S.-H. Oh, S.-J. Im, S. Jeong, A. Jang, Nanoparticle charge affects water and reverse salt fluxes in forward osmosis process, Desalination, 438 (2018) 10-18.

[16] J. Wang, T. Xiao, R. Bao, T. Li, Y. Wang, D. Li, X. Li, T. He, Zwitterionic surface modification of forward osmosis membranes using N-aminoethyl piperazine propane sulfonate for grey water treatment, Process Safety and Environmental Protection, 116 (2018) 632-639.

[17] H.-R. Zuo, J.-B. Fu, G.-P. Cao, N. Hu, H. Lu, H.-Q. Liu, P.-P. Chen, J. Yu, The effects of surface-charged submicron polystyrene particles on the structure and performance of PSF forward osmosis membrane, Applied Surface Science, 436 (2018) 1181-1192.

[18] G. Xie, W. Xu, Q. Ge, Controlling membrane ionization with bifunctional alendronates to benefit desalination through forward osmosis, Desalination, 447 (2018) 147-157.

[19] L. Setiawan, R. Wang, K. Li, A.G. Fane, Fabrication of novel poly(amide–imide) forward osmosis hollow fiber membranes with a positively charged nanofiltration-like selective layer, Journal of Membrane Science, 369 (2011) 196-205.

[20] C. Bellona, J.E. Drewes, The role of membrane surface charge and solute physico-chemical properties in the rejection of organic acids by NF membranes, Journal of Membrane Science, 249 (2005) 227-234.

[21] N. Qi, P. Wang, C. Wang, Y. Ao, Effect of a typical antibiotic (tetracycline) on the aggregation of TiO2 nanoparticles in an aquatic environment, J Hazard Mater, 341 (2018) 187-197.

[22] S.-z. Li, X.-y. Li, D.-z. Wang, Membrane (RO-UF) filtration for antibiotic wastewater treatment and recovery of antibiotics, Separation and Purification Technology, 34 (2004) 109-114.

[23] S.-F. Pan, M.-P. Zhu, J.P. Chen, Z.-H. Yuan, L.-B. Zhong, Y.-M. Zheng, Separation of tetracycline from wastewater using forward osmosis process with thin film composite membrane – Implications for antibiotics recovery, Separation and Purification Technology, 153 (2015) 76-83.

[24] E.M. Hotze, T. Phenrat, G.V. Lowry, Nanoparticle Aggregation: Challenges to Understanding Transport and Reactivity in the Environment, Journal of Environmental Quality, 39 (2010) 1909-1924.
[25] R.A. French, A.R. Jacobson, B. Kim, S.L. Isley, R.L. Penn, P.C. Baveye, Influence of Ionic Strength, pH, and Cation Valence on Aggregation Kinetics of Titanium Dioxide Nanoparticles, Environmental science & technology, 43 (2009) 1354-1359.
[26] B.J. Thio, D. Zhou, A.A. Keller, Influence of natural organic matter on the aggregation and deposition of titanium dioxide nanoparticles, J Hazard Mater, 189 (2011) 556-563.
[27] S. Phuntsho, S. Vigneswaran, J. Kandasamy, S. Hong, S. Lee, H.K. Shon, Influence of temperature and temperature difference in the performance of forward osmosis desalination process, Journal of Membrane Science, 415-416 (2012) 734-744.
[28] X. Song, Z. Liu, D.D. Sun, Nano gives the answer: breaking the bottleneck of internal concentration polarization with a nanofiber composite forward osmosis membrane for a high water production rate, Adv Mater, 23 (2011) 3256-3260.
[29] D.J. Shaw, 8 - Colloid stability, in: D.J. Shaw (Ed.) Introduction to Colloid and Surface Chemistry (Fourth Edition), Butterworth-Heinemann, Oxford, 1992, pp. 210-243.
[30] D.J. Shaw, 7 - Charged interfaces, in: D.J. Shaw (Ed.) Introduction to Colloid and Surface Chemistry (Fourth Edition), Butterworth-Heinemann, Oxford, 1992, pp. 174-209.
[31] W. Liu, W. Sun, A.G.L. Borthwick, J. Ni, Comparison on aggregation and sedimentation of titanium dioxide, titanate nanotubes and titanate nanotubes-TiO2: Influence of pH, ionic strength and natural organic matter, Colloids and Surfaces A: Physicochemical and Engineering Aspects, 434 (2013) 319-328.